Space Rider Re-Entry Module Scaled Down Flight Test Campaign

J. Cardín[(1)], H. Gutiérrez[(1)], G. Rodríguez[(1)], A. Fernández[(1)], J. Sintes[(1)], M. Lucrezia[(1)], J. Ramírez[(1)], F. Cacciatore[(1)], D. Bottero[(2)], G. Curti[(3)]

[(1)] SENER Aeroespacial, C/Severo Ochoa 4, Tres Cantos, 28760, Spain, jorge.cardin@aeroespacial.sener
[(2)] Thales Alenia Space Italy, Str. Antica di Collegno, 253, 10146 Torino TO, Italy, davide.bottero@thalesaleniaspace.com
[(3)] ESA-ESRIN, Via Galileo Galilei, 1, 00044 Frascati RM, Italy, gianluca.curti@esa.int

ABSTRACT

In the context of the Space Rider verification campaign a set of drop tests are planned to characterize the real behaviour of the system and GNC under parafoil. To lower the cost and risk associated to this activity, a Scaled Down Flight Test campaign is designed to consolidate the GNC maturity, get a preliminary performance assessment and tune the tools and procedures that will be used to characterize the full-scale system.

SENER Aeroespacial is responsible of the design, integration, and testing of such scaled-down vehicle together with the identification tools. The vehicle is currently in the finishing the integration phase, aiming to perform the flight campaign in the summer of 2023. The parafoil aerodynamic identification algorithms and the expected scaled system GNC performances have been evaluated in a simulated environment tailored from the Space Rider Parafoil GNC design simulator.

1 INTRODUCTION

Space Rider (SR) programme aims to provide Europe with a reusable platform for in-orbit operations. Each of its planned missions consists of a launch and orbit injection phase, up to six months of in-orbit operation and then an autonomous re-entry, descent and landing. During the landing phase the control is achieved using a parafoil, enabling trajectory tracking and precision landing capabilities.

As the flight under parafoil is an unpowered phase, the control authority is low and subject to atmospheric disturbances. For this reason, it is critical to have a well stablished understanding of the plant and system response. To improve this knowledge and the representativeness of the simulation models used to characterize the system, a series of System Drop (SD) tests is envisioned, both in open loop and closed loop. However, due to the high cost associated to these tests, a Scaled Down Flight Test (SDFT) campaign is proposed to reduce cost and risk associated to the first flight tests.

This paper describes and justifies the design of the SDFT vehicle, informally named Starling, that will be used to develop and test the tools for SD campaign and exercise the SR Guidance Navigation and Control (GNC) algorithms of the landing phase, including the Parafoil GNC (PGNC) and Model Predictive Control (MPC) used for the flare manoeuvre, in a representative environment with reduced cost and risk.

The SDFT and its vehicle are designed, developed and operated by SENER Aerospacial within the frame of the ESA Space Rider Reentry Module GNC development, for which SENER is GNC Design Authority under contract with TAS-I.

Starling design is based on COTS elements. The vehicle is composed by paratrike as main frame and a parafoil to provide lift to the system. A paramotor is added to provide thrust during the climbing phases; and a set of winch actuators to control the parafoil shape and steer the system. The control can be commanded both by a remote operator through a radio controller or autonomously by the onboard avionics. The remote pilot will always have full authority over the control to allow recovering the system in case of GNC failure. The avionic box includes a set of sensors required by the GNC algorithms to control the system and some ancillary sensors that will be used to identify and characterize the system behaviour during flight.

Due to its characteristics, Starling falls into the Precision Aerial Delivery Systems (PADS) category. This kind of system has been studied since the 1960s as a mean of delivering a wide range of unpowered payloads in different scenarios. One of the closest use cases to the SDFT is that of Buckeye [10][11], the scale-down demonstrator of the NASA's X-38 program. In the same context of parafoil guided landing for space vehicles, the DLR developed the technology demonstrator ALEX (100kg) in the late 1990s [12]. In the military sector, the US Army has also dealt with this type of system with the SnowFlake (2kg), SnowBird (60kg) and SnowGoose (270kg) vehicles developed by MMIST [13] and the UK Navy has selected Animal Dynamics' Stork (135kg) for the Royal Navy's Uncrewed Aerial Systems Heavy Lift Challenge.

2 SDFT SYSTEM DESCRIPTION

Aiming at limiting the cost and time span of the SDFT integration, Starling is based on COTS elements, including a paratrike capable of lifting up to 250kg, adapted to be controlled either remotely (via RC controller) or autonomously with the integrated avionics and sensors. The design of this vehicle heavily exploits SENER's experience obtained by developing SPADS, a 25kg PADS system used as technology demonstrator for PGNC algorithms [2]. The elements and units composing the system are listed in Table 2-1 and can be grouped in two main groups:

1. Elements required to fly the vehicle: trike, parafoil, actuators (winches and propeller), remote controller, FPV goggles, FPV camera and main onboard computer
2. Avionics required to fly autonomously and record the system state: sensors and avionic onboard computer

This distinction has the purpose of isolating the critical elements required to fly in a safe manner, both from a logical and physical point of views. This approach is selected based on the relatively high computational load that the avionics computer will have as it will manage the GNC algorithms, sensor processing and data recording. In this sense, it is preferable to have an additional system computer exclusively dedicated to the operation of the vehicle, reducing the risk of freezing or getting stuck causing a mission failure.

A visual representation of the elements composing the control system and avionics is depicted in Figure 2-1. Figure 2-2 presents a mock-up for the avionic box, including the elements required for the autonomous flight.

Table 2-1: SDFT Components

Unit	Comment	Scope
Vehicle		
Paratrike	See Table 2-2	Global
Engine	2stroke engine, 38CV 140cm 2blade propeller	Manual flight
Parafoil	310ft^2, glide ratio 3.5-4:1	Global
Winches	Rated torque 18Nm Max. speed 26rad/s	Global
System Computer	COTS board	Global
Parachute	Ballistic Parachute	Safety
Avionics		
Avionics Computer	COTS board, same as System Computer	Autonomous flight
Navigation unit	GNSS + IMU	Autonomous flight System Identification
Altimeter	Range: 1.0-500.0m	Autonomous flight
Air Data System	Max: 1psi Resolution: 0.84Pa	System Identification
Power system	10Ah, 22.2V	Global
Controller	Remote camera DJI googles 2 + remote controller 2	Manual flight
Monitoring	Camera to capture behaviour of all flying elements	System Identification

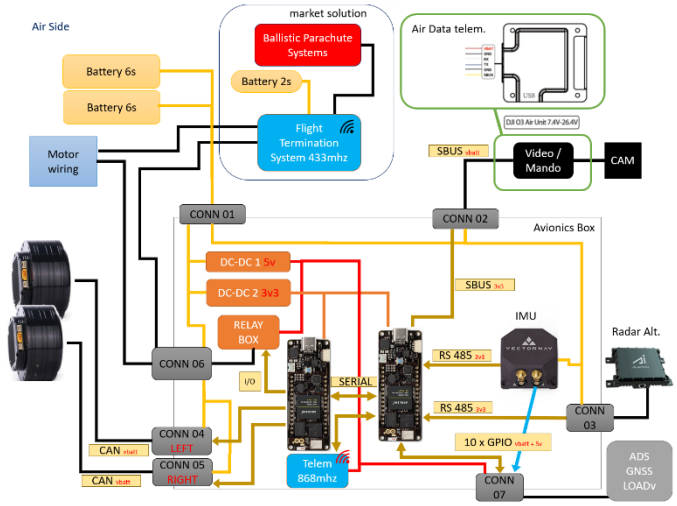

Figure 2-1: Hardware Architecture

Figure 2-2: Avionics Mock-up

Starling's parafoil is provided by CIMSA, the same producer of the Space Rider full size parafoil. The parafoil will have the characteristics summarized in Table 2-2, aiming to show the same wing profile as the SR flight parafoil to maximize the representativeness of the flying qualities.

The winch motors have been sized assuming a requirement of line tension equivalent to 10% of the total suspended mass, and capable of with a displacement of 0.5 m at a speed of 1m/s. Such speeds provide more than enough margin to represent the actual SR winch performance. The winches, then, are composed of a low and high torque brushless motor, with a planetary gearbox. The motor has a controller board, connected via CANbus to the Arduino, which allows it to operate in servo mode. A disk is attached to the motor, which will wind up the control line of the parafoil.

Table 2-2: CIMSA Plus 310 parafoil data, from [4]

Plain shape	Rectangular
Area (ft2)	310
Nº of cells	9
Span (m)	8.82
Chord (m)	3.27
Aspect ratio	2.7
Max. Wing Load (lb/ft2)	1.06 for mass of 150 kg
Min. Wing Load (lb/ft2)	0.71 for mass of 100 kg
Gliding ratio	3.5-4:1

Figure 2-3: CIMSA Plus 310 profile

3 SOFTWARE

The SDFT SW manages the vehicle when it is remotely operated. It receives the pilot commands via the remote controller and controls the paramotor and the winches. It runs in the Trike Arduino which communicates with the avionics Arduino to receive and execute winch actuations while in autonomous mode. The interface used for the winches motors is CAN bus, and the interface with the remote controller is sBus. The software is managed in a robust manner, as the critical functions to control the vehicle in manual mode are executed in its own Arduino, as well as switching between manual and autonomous mode. In addition, each Arduino has its own M4 processor, with a lower performance than the main M7 processor, that can be used to free some tasks to the main processor.

Following the distinction between the system and avionics onboard computers, two software elements are defined each unit separately:

- **Platform software**: Manages the vehicle when it is remotely operated. It receives the pilot inputs via the remote controller and commands the paramotor and the winches. It runs in the system computer and is also connected to the avionics to receive and execute winch actuations while in autonomous mode.
- **Application software**: Manages the vehicle in autonomous mode. It includes a scheduler that operates the sensor drivers, performs the data logging, execute the GNC algorithms and communicates with the system computer. This software is loaded in the avionics computer and is executed in real time.

A basic function allocation and interconnection is presented in Figure 3-1.

3.1 Application SW

This is the SW in charge of the autonomous part of the flight and manages the main functions of the avionics. The ASW is composed by:

- **Scheduler**: It manages the execution of the different functions, gathers, and stores the data from the sensors (IMU+GNSS and radar altimeter modules) via drivers. It also communicates with the trike Arduino. This SW runs in real time.
- **GNC**: An autocoded version of the SR-GNC Matlab algorithms tuned for Starling
  - **PGNC**: Algorithms for trajectory tracking under parafoil
  - **MPC**: Optimal guidance and control algorithms to minimize the touch down velocities
- **Support SW**: Any ancillary SW not covered by previous items.

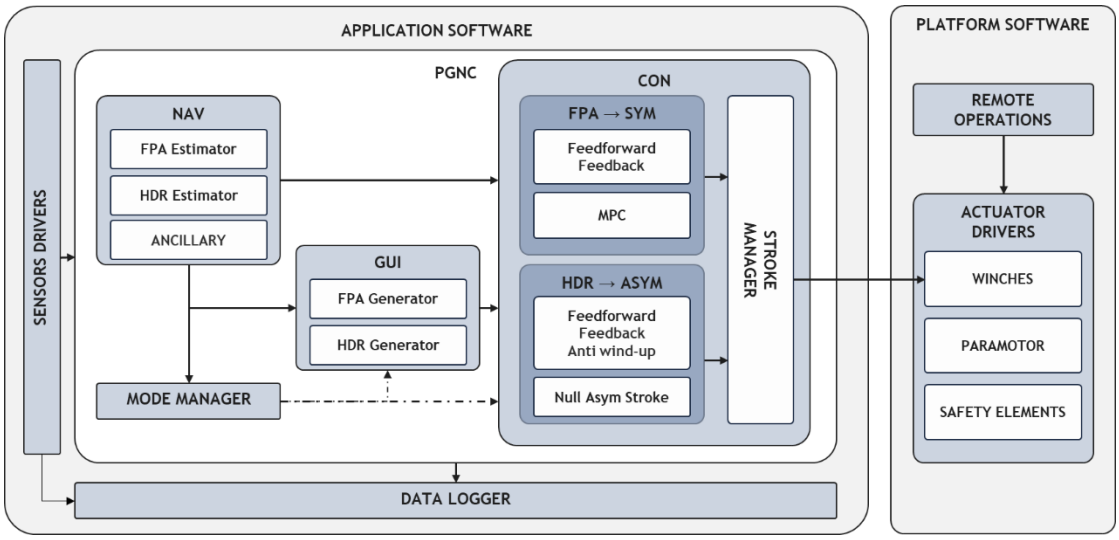

Figure 3-1: Software Architecture

3.2 GNC algorithms

The GNC algorithms loaded in the avionics computer are an autocoded version of the PGNC algorithms developed in Matlab for the SR reentry mission, so they are fully representative of the full-scale system. Only the mission parameters related to trajectory planning and the control tuning are adapted to better match the SDFT needs.

From an operative point of view, once the remote pilot transfers the authority to the onboard computer and the PGNC, the vehicle will follow the Space Rider's parafoil guidance laws. The vehicle will fly towards the landing site and define the energy management spiralling down pattern around it. Once the PGNC computes a feasible trajectory, it will perform a terminal guidance manoeuvre to approach the landing point along the headwind direction. Back-up logics are placed in case this condition is not met, allowing to reach the landing point from any direction.

The last phase before landing is a flare manoeuvre designed to minimize the vertical impact velocity at touchdown. During this phase a MPC algorithm is activated to excite the dynamic longitudinal response of the system and reach vertical velocities outside the trimmed conditions. This algorithm is further explained in [3].

In terms of architecture, the PGNC is divided in two control loops: one for the longitudinal motion that actuates over the Flight Path Angle (FPA) commanding symmetric strokes; and one for the lateral motion that actuates over the Heading Rate (HDR) commanding asymmetric strokes. On top of that, a set of navigation functions compute the current state of the system and some ancillary signals required by the guidance and the mode manager algorithms. Refer to [1] for a detailed description of Space Rider's PGNC design.

4 OPERATIONS

As previously introduced, the vehicle is designed to fly both in manual and autonomous regimes. The nominal mission profile consists of a sequence of remotely controlled powered climbs, followed by the proper test phase in which the system will glide autonomously using either a predefined winch command history in open loop or the outputs of the PGNC algorithms in closed loop. Once the test is finished, and before touching down, the pilot will recover the control, throttle up the propeller and perform an addition climb. This allows to perform several tests without going through the critical

take-off and landing phases. Once the tests campaign is completed or the system is running out of fuel/power, the pilot will regain the control and land manually (unless the test is devoted to test the flare manoeuvre). The nominal test sequence is depicted in Figure 4-1.

The remote pilot shall always control the powered flight phases (i.e, take-off and climb) to reduce the risk associated to the extended range achieved by the propeller action. In addition, the pilot has full authority over the autonomous phases and can recover the system control at any point in time.

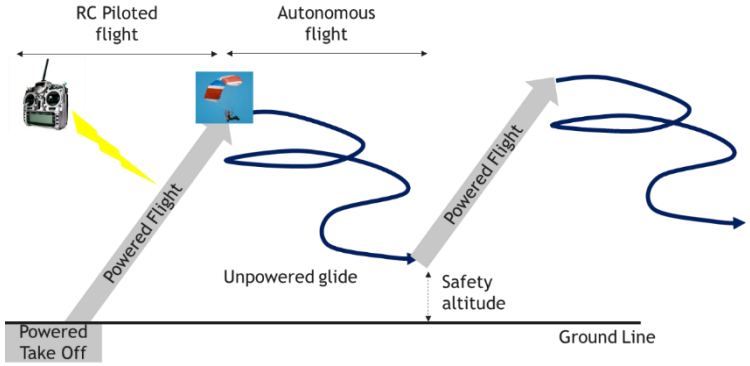

Figure 4-1: SDFT Nominal Mission Profile

4.1 System modes

To cycle between the different configurations associated to the different tests, the system computer defines the modes depicted in Figure 4-2.

- **Manual (LoS/FPV)**: The pilot has complete control over the system. The vehicle is controlled by the pilot using direct Line of Sight (LoS) or using a First Person View (FPV) headset. These are the only modes where throttle level can be adjusted.
- **Autonomous**: The parafoil commands are generated by the avionics computer. This mode accepts commands generated in open loop and close loop.
- **Safe**: The communication between pilot and vehicle is lost. The vehicle will command a spiralling manoeuvre to land as soon as possible while reduce the distance covered without command
- **Emergency**: The actuation is lost. The vehicle will deploy the safe measures (parachute) and land as soon as soon as possible.

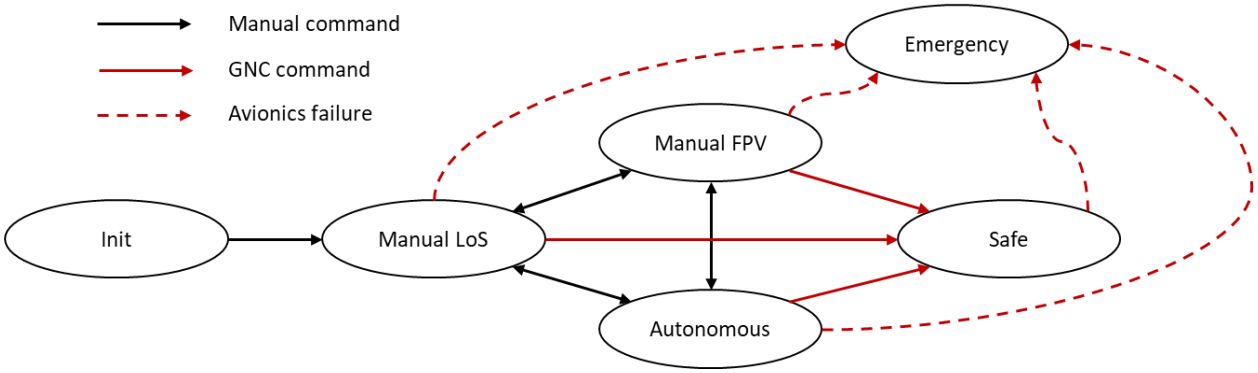

Figure 4-2: SDFT Operative Modes

4.2 Test campaign

The complete SDFT campaign is divided in 4 stages according to the type and goal of the test. This distinction has an operative purpose: Each stage has different flight envelopes and associated risks, imposing increasing restrictions on the test ranges in which they can be executed.

1. **Stage I – Integration & debugging tests**: intended to test all functionalities in a staggered approach, ensuring at each step that the required functionality is working and is safe to use, with the main objective to validate the vehicle integration, operability, and manoeuvrability. If everything is ok, then the System identification flight test can start.
2. **Stage II – System identification**: envisaged to complete the system identification tests. The main objective is to gather the maximum information of the flights performances and environment to characterize the system. Each flight will perform several manoeuvres, the more flight tests executed the better statistical representativeness.
3. **Stage III – GNC tuning:** start the tuning loop and PGNC/MPC Flight tests. All modes/phases will be executed independently.
4. **Stage IV – GNC performance:** envisioned for E2E flight tests, from different initial conditions in terms of altitude, distance, wind direction, different WP1 locations, etc.

All the flight tests are planned to be carried out during the summer of 2023 in Spain. The following candidate test sites are planned for the tests:

Table 4-1 Test sites selection

Test Stage	Max Altitude	Main	Backup
I-II	500m	Uceda	CENAD San Gregorio
III-IV	1500m (TBC)	CENAD San Gregorio	ATLAS

Uceda test range, located north of Madrid, has a size of approximately 4.5 x 6 km, and will be used for flights below 500 m altitude approximately. The Uceda test range is usually used by Spanish armed forces for parachute drops exercises. The CENAD San Gregorio is a National Training Center of the Spanish Army. It's located near Zaragoza, Spain. The test range area has a longer span of approximately 28 km length. The area is used for mechanized units training, tactical exercise, combat vehicles training, shooting exercises. ATLAS (Air Traffic Laboratory for Advanced unmanned Systems) is a Test Flight Centre located in Villacarrillo (Jaen) which offers the international aerospace community an aerodrome equipped with excellent technological-scientific facilities and airspace ideally suited to the development of experimental flights with unmanned aerial vehicles (UAS/RPAS). The ATLAS Centre holds the first facilities in Spain exclusively dedicated to testing light and tactical Unmanned Aircraft System (UAS) or Remotely Piloted Aircraft Systems RPAS.

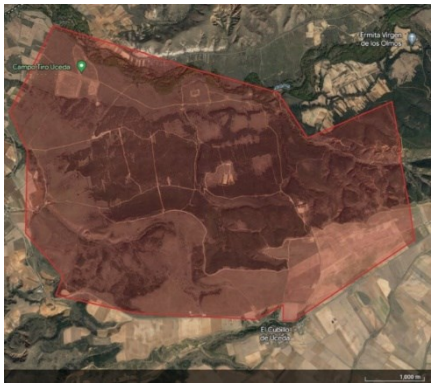

Figure 4-3: Uceda test range

Figure 4-4: CENAD San Gregorio location

5 SYSTEM IDENTIFICATION

One of the main goals of the SDFT campaigns is the development of tools that allow the identification of the system behaviour during flight. These tools aim to improve the representativity of the models used to tune the GNC and evaluate its performance in a simulated environment. The main focus of this activity is to obtain a test-based estimation of the parafoil Aerodynamic Database (AEDB) and to consolidate the dispersion level associated to the parafoil flight performance.

In this sense, similar activities have been performed within the framework of X-38 program, where a trimmed parafoil was always considered for the analysis on the longitudinal dynamics [5], and only the yawing motion was characterized for the lateral dynamics [6]. In addition, also within the context of the X-38, the author in [7] applied the Observer/Kalman Filter Identification (OKID) method to identify a linear model for the Buckeye system assuming periodic disturbances. Then, in reference [8] efforts were done on the identification of the steady-state lift, drag and turn rate to generate a simulation model from the observation of the steady-state system response.

In this case, both the steady-state and the transient are observed to characterize the parafoil-vehicle dynamics more accurately. Moreover, all six coefficients (i.e., drag, lateral, lift, roll, pitch, and yaw) are to be identified to generate a full 6DOF simulation model. Then, based on the data recorded during the flight campaigns, the identification process will model:

- The aerodynamic coefficients required by the simulated aerodynamic model
- The degree of parafoil-payload relative motion

5.1 Aerodynamic database

Due to the high influence of the aerodynamic characteristics of the parafoil in the system behaviour, it is of paramount importance to use a representative model during the GNC development. For this reason, a dedicated aerodynamic database identification loop was deemed necessary to raise the confidence of the simulated results.

The identification involves 3 steps:

1. **Data acquisition** from the flight tests: recording the system state, control commands and environmental conditions experienced by the system.
2. **Data processing** to compute the desired magnitude: in this case, the total aerodynamic coefficients
3. **Data refinement**: Apply filtering and estimation to estimate partial derivatives, remove errors, noises, and cross-dependencies

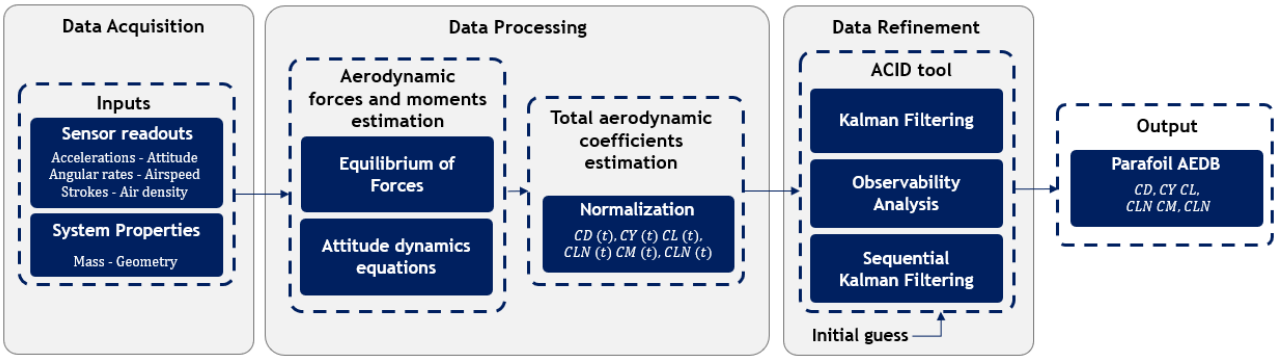

Figure 5-1: AEDB Identification Flow

Data acquisition

Table 5-1 specifies all the recorded signals required for the aerodynamic characterization together with the measuring sensor and the accuracies assumed in the results presented in §6.3.

Table 5-1: AEDB Identification Data Acquisition

Element	Measurement	Sensor	Accuracy 3σ
Trike	Acceleration	IMU (NAV Unit)	18.3 mm/s^2
Trike	Velocity	NAV Unit	6 cm/s
Trike	Attitude	NAV Unit	0.1 deg
Trike	Angular rate	IMU (NAV Unit)	7.2e-2 deg/s
Trike	True Airspeed	Pitot tube	1 m/s
Trike	Density	Pitot tube	6.7e-3 kg/m^3
Trike	Angle of Attack	Pitot tube (config.)	0.5 deg
Trike	Angle of Sideslip	Pitot tube (config.)	0.5 deg
Parafoil	Winches position	Winch motor encoder	0 mm
Parafoil	Attitude	IMU / Camera	0.1 deg
Parafoil	Angular rates	IMU	0.01 deg/s

Data processing

Using the sensor readouts, and assuming that the system behaves as a 6DOF rigid body, it is possible to compute the total aerodynamic coefficients by using the equilibrium of forces and moments (Eqs. 1-2) together with the definition of the aerodynamic actions (Eqs. 3-4). These equations consider that the aerodynamic forces of the trike and the effect of the suspension lines are negligible.

$$\boldsymbol{F}_{aero,pf/FB} + \boldsymbol{F}_{g,sys/FB} = m_{sys}\ddot{\boldsymbol{x}}^{i}_{sys/FB} \tag{1}$$

$$\boldsymbol{M}_{aero,pf/FB} = I_{sys}\dot{\boldsymbol{\omega}}^{i}_{sys/FB} + \boldsymbol{\omega}^{i}_{sys/FB} \times I_{sys}\boldsymbol{\omega}^{i}_{sys/FB} \tag{2}$$

Where ($\boldsymbol{F}_{aero,pf/FB}$, $\boldsymbol{M}_{aero,pf/FB}$) are the aerodynamic forces and moments; $\boldsymbol{F}_{g,sys/FB}$ is the weight of the system including trike and parafoil; (m_{sys}, I_{sys}) are the mass and inertia of the system; and ($\ddot{\boldsymbol{x}}^{i}_{sys/FB}$, $\dot{\boldsymbol{\omega}}^{i}_{sys/FB}$, $\boldsymbol{\omega}^{i}_{sys/FB}$) are the system linear acceleration, angular acceleration and angular velocity expressed with respect an inertial frame of reference. Note that all the elements of these equations are expressed in Flight Body (FB) frame, which is a geometric frame centred at the Centre of Gravity (CoG) of the system with X-forward, Y-left, Z-down.

Normalizing the aerodynamic forces and moments with the atmospheric density (ρ), parafoil airspeed ($V_{air,pf}$) and parafoil area (S_{pf}), span (b) and chord (c); the total aerodynamic coefficients become:

$$\begin{bmatrix} C_A \\ C_Y \\ C_N \end{bmatrix} = \frac{2\boldsymbol{F}_{aero,pf/FB}}{\rho S_{PF} V^2_{air,pf}} \cdot \begin{bmatrix} -1 \\ 1 \\ -1 \end{bmatrix} \tag{3}$$

$$\begin{bmatrix} C_{LL} \\ C_M \\ C_{LN} \end{bmatrix} = \frac{2\boldsymbol{M}_{aero,pf/FB}}{\rho S_{PF} V^2_{air,pf}} \cdot \begin{bmatrix} 1/b \\ 1/c \\ 1/b \end{bmatrix} \tag{4}$$

Data refinement

At this point, the user has a measurement of total aerodynamic coefficients and the control and air states at each instant. To get one step further and get the partial coefficients required by the aerodynamic model, a dedicated Aerodynamic Coefficients IDentification (ACID) tool is developed.

The tool is based on Kalman filtering for constant estimation. In this sense, the user must specify the structure of the aerodynamic model and a first estimation of the total coefficients. Then a least squares problem is solved recursively to compute the parameters of the parametrized equations.

Since there are several parameters to be identified, the observability of these may be a concern, as one parameter might shadow the influence of others on the overall system response. For this reason, an observability analysis is performed a posteriori from the first estimation [9] and then, the list of parameters to be identified is divided into several subsets and estimated separately with sequential Kalman filters.

The final implementation is based the following sequence:

1. Kalman filtering for constants estimation over a single total coefficient, using each readout as an independent measurement
2. Sensitivity analysis to assess the contribution of each parameter over the estimated coefficients and collinearity analysis to evaluate the correlation between the different parameters
3. Subset generation, grouping coefficients with collinearity below a predefined threshold to ensure generated values are independent
4. Sequential Kalman filter over the independent subsets, fixing the coefficients outside the study to limit their influence. This step is repeated until convergence is reached.

5.2 Parafoil-Payload relative motion

As previously stated, the simulator environment used to develop and test the GNC algorithms assumes a 6DOF dynamic response, meaning that the payload-parafoil system behaves as a single rigid body. This modelling choice follows the indications of the Space Rider parafoil provider; in addition, even if the GNC algorithms are developed on 6DOF models, the resulting behaviour and performance are crosschecked both in 6DOF (Functional Engineering Simulator, FES) and 12DOF (NUMES, developed by TASI) simulators. To verify the 6DOF motion assumption the relative motion between parafoil and platform is measured during the scaled flight tests.

Two different approaches are envisioned for such estimation:

- **Navigation units**: Measuring the relative motion between 2 IMUs, one installed in the payload and another in the parafoil.
- **Optical:** Using optical elements such as the ArUco markers show in Figure 5-2 and a camera to record the relative motion.

On the visual approach, a video camera is mounted onboard the platform pointing upwards to observe the markers sticked on the canopy. Then, the video data gathered during the tests flights is post-processed to detect the optical elements and compute their relative position and attitude with respect to the camera. Finally, the attitude of the parafoil is estimated computing the mean attitude quaternion from the single markers attitude estimation.

Figure 5-2: Parafoil Attitude Estimation with ArUco Markers

6 SIMULATIONS

At the moment of writing this paper the vehicle is still under development, with the first set of shakedown tests planned for the last week of May 2023. In order to test the algorithms and tools before applying them to the real flight environment, a set of simulations are carried out using the SR simulator facility with scaled properties.

6.1 Model description

The simulator inherited from SR considers the parafoil-payload system a 6DOF rigid body and includes the following effects in the propagation:

- Parafoil and payload mass properties
- Parafoil and payload aerodynamics
- Earth gravity
- Atmospheric conditions
- Winds, including temporal effects, turbulence, and updrafts
- Propagation in ECI, ancillary signals in ECEF, local vertical and geometric body frames.

As the parafoil selection of Staling tries to mimic the SR dynamic response, the same structure is assumed for the aerodynamic model of the parafoil. In this sense, the same aerodynamic model is used for the first set of simulations.

Several of the vehicle properties will not be known until the system is fully integrated and the parafoil is rigged for flight. To simulate the vehicle and get a preliminary assessment of the dynamic response and GNC performances the missing dimensions are generated using a scaled down version of SR geometry. The scaled parameters used in the simulator are listed in Table 6-1. All these parameters will be reviewed and updated once the vehicle integration is completed.

Table 6-1: Scaled Parameters for SDFT Simulator

Parameter	Scaling Approach
System mass	Vehicle specification
System inertia	Scaled with vehicle mass
System centre of gravity	Scaled with parafoil span
Parafoil span	Parafoil specification
Parafoil surface	Parafoil specification
Parafoil aspect ratio	Equal by design
Aerodynamic model	Equal by design
Winch stroke range	Scaled with parafoil span
Suspension line geometry	Scaled with parafoil span
Sensor placement geometry	Scaled with parafoil span

6.2 SDFT performance

Using the aforementioned simulator, a series of open loop manoeuvres are executed using Starling and SR configurations. Figure 6-1 and Figure 6-2 show the dynamic response of both systems to the maximum symmetric and asymmetric pulls. Table 6-2 and Table 6-3 summarize the main performance metrics.

Table 6-2: Longitudinal Response Starling vs. SR

Initial Stroke		Final Stroke		Δ FPA (deg)		Settle time 2% (s)	
Sym	Asym	Sym	Asym	SR	SDFT	SR	SDFT
MIN	NULL	MID	NULL	-2.1	-2.5	~21	~19
MIN	NULL	MAX	NULL	-5.9	-6.4	~22	~20

Table 6-3: Lateral Response Starling vs. SR

Initial Stroke		Final Stroke		HDR (deg/s)		Δ Roll (deg)		Settle time 2% (s)	
Sym	Asym	Sym	Asym	SR	SDFT	SR	SDFT	SR	SDFT
MID	NULL	MID	MID	3.1	8.4	3.2	8.2	~9	~6
MID	NULL	MID	MAX	7.9	23.3	8.2	23.4	~12	~9

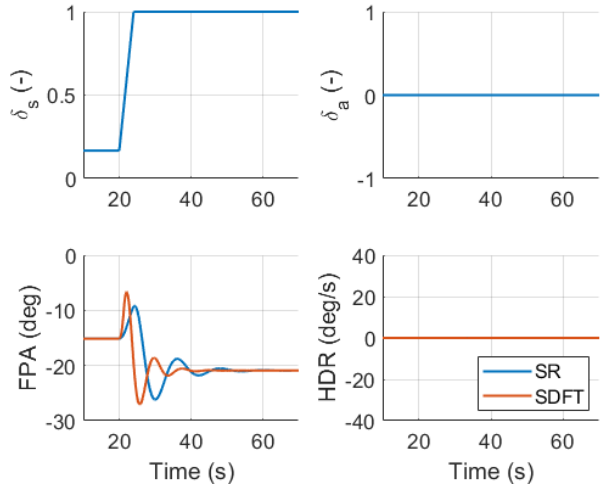

Figure 6-1: Response to max. sym pull Starling vs. SR

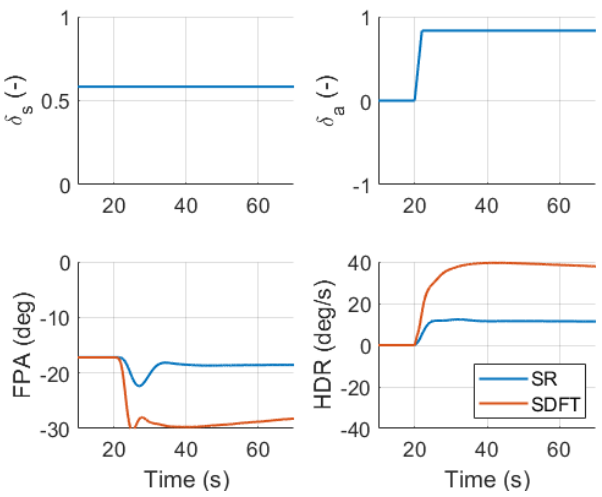

Figure 6-2: Response to max. asym. Pull Starling vs. SR

This analysis shows that Starling is more reactive to the control inputs than SR, achieving faster heading rates in shorter times for the same command. Figure 6-3 shows the steady state response for different left/right stroke pairs and the response envelope for each vehicle. Instead of exploiting the full envelope, the GNC algorithms loaded in the SDFT will limit the commands to stay within the SR envelope, maximizing the representativeness of manoeuvres executed by the GNC.

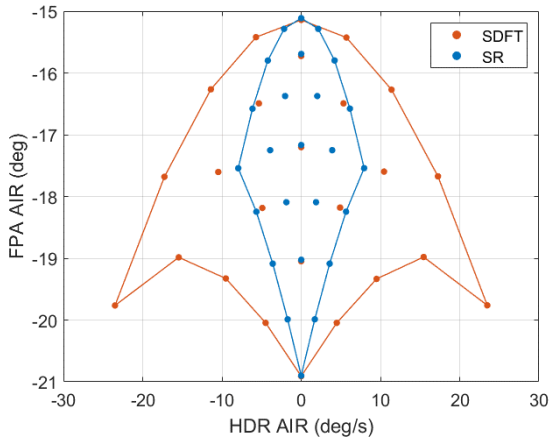

Figure 6-3: Command Envelope SDFT vs. SR

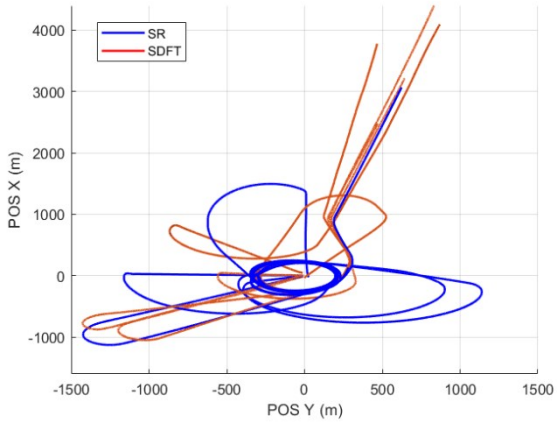

Figure 6-4: PGNC Trajectories SDFT vs. SR

After confirming that Starling's actuation envelope contains the one of SR, the PGNC algorithms are tested in a Monte Carlo campaign to assess the general behaviour. After performing one tuning loop of the control algorithms to account for the different mass range, Starling and SR responses to the PGNC are simulated in the same conditions for comparison (see Figure 6-4). The results show that trajectories of Starling and SR are statistically equivalent, confirming the representativeness of the SDFT campaign for the SR PGNC behaviour.

6.3 ACID Tool

The simulator is also used to test the ACID tool in a controlled environment to quantify the accuracy of the estimator. This metric is critical, as it can be used to estimate the error of the onboard performance models used by the GNC which are one of the main contributors to the landing accuracy.

As introduced in §5.1, the ACID tool works over an aerodynamic model that should be specified by the user, in this case the structure of the simulated aerodynamic model is fed to the tool.

The evaluation of the tool performance is performed following the same steps described in §5.1. For this analysis a nominal aerodynamic database is considered as reference.

- **Data acquisition**: A set of open loop simulations are executed using a set of "real" aerodynamic coefficients (reference database plus dispersion to simulate uncertainty).
- **Data processing**: The simulated outputs are processed to generate the total aerodynamic coefficient history.
- **Data refinement**: The coefficient history is fed to the ACID tool together with the reference (unperturbed) aerodynamic database, which is used as initial guess

The accuracy of the tool is then the difference between the estimated coefficients and the ones used by the simulator. For an effective estimation, starting from the reference aerodynamic database, the tool shall compute the perturbed database. Figure 6-5 and Table 6-4 serve as an example of the estimation process over the drag coefficient. In this case 3 different manoeuvres are simulated varying the symmetric stroke.

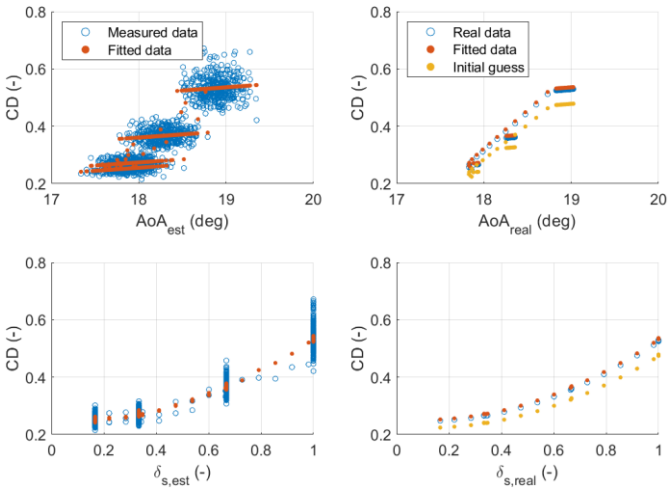

Figure 6-5: ACID CD Results I

Table 6-4: ACID CD Results II

Coeff	Sim	Init	Final
$C_{D,0}$	0.0111	0.0100	0.0134
C_{D,α_1}	0.1346	0.1216	0.1123
C_{D,α_2}	2.0164	1.8213	1.7746
$C_{D,\delta_{s_0}}$	-0.0009	-0.0008	0.0300
$C_{D,\delta_{s_1}}$	-0.0505	-0.0456	-0.0404
$C_{D,\delta_{s_2}}$	0.3032	0.2739	0.3004
ΔC_D (%)	-	6.48%	1.14%

One important remark is that, although the direct comparison of each partial coefficient shows a degradation after the estimation compared to the initial guess, the relevant metric is the fitness of the total coefficient curve over its applicability range, which is significantly improved.

The accuracy of the estimation is highly dependent on the studied manoeuvres since it is important that the proper states of the system are excited enough. A set of asymmetric manoeuvres are used identify the lateral coefficients, and the same process is repeated for every aerodynamic coefficient. The results obtained for the different coefficients are summarized in Table 6-5:

Table 6-5: ACID Errors

Scope	ΔC_D (%)	ΔC_Y (%)	ΔC_L (%)	ΔC_{LL} (%)	ΔC_M (%)	ΔC_{LN} (%)
Initial	6.48%	3.33%	9.53%	0.90%	81.90%	9.65%
Final	1.14%	0.53%	0.53%	0.77%	0.94%	0.31%

As can be noted the achieved error over the total aerodynamic coefficients is below 1.5% for all contributions. Specially, the pitch coefficient, that even though it initially has a high mean dispersion, it is reduced to an error below 1%. It can be also observed that in the case that the initial guess has a low error with respect to the "real" database, as it is for the roll coefficient, the accuracy is not degraded.

7 CONCLUSIONS

The SDFT campaign is planned as a de-risking activity in the context of the SD test for the SR reentry mission. This paper presented the main advances performed in this context, both in the Starling design and in the development of the tools that will be used to postprocess the flight data.

In particular, a broad description of Starling architecture, avionics and software elements have been presented. The operative plan envisions a stepped test campaign, which is expected to start by the end of May 2023 with the first flights.

To mitigate the risks associated to the first flights, a series of simulations have been carried out to get a preliminary metrics on the expected system performance based on scaled down properties. This

same simulator serves as design and verification environment for a in-house aerodynamics identification tool that will be used to characterize Starling and SR real aerodynamics and refine the simulation models.

8 REFERENCES

[1] Cardín J. et al, *Space Rider Re-Entry Module: Gnc Design And Development For Europe's Reusable Space Transportation System,* IAC-22-D2.3.2, Paris 2022

[2] Cardín J. et al, *SPADS: design and in-flight demonstration of a precision landing parafoil system,* IAC-22-D2.6.3, Paris 2022

[3] Ramírez J., et al, *Embedded Optimization for Space Rider Reentry Module Parafoil GNC,* ESA GNC-ICATT, 2023

[4] CIMSA, *Personnel Military Systems, Plus Heavy Duty Tactical Canopies*, http://www.cimsa.com/pdf/parachute/PLUS_BP_ENG_2021.pdf

[5] Schroeder Iacomini C., and Cerimele C.J., *Longitudinal Aerodynamics from a Large Scale Parafoil Test Program*, AIAA 99-1732, 15th AIAA Aerodynamic Decelerator Systems Technology Conference and Seminar, June 1999.

[6] Schroeder Iacomini C., and Cerimele C.J., *Lateral-Directional Aerodynamics from a Large Scale Parafoil Test Program*, AIAA 99-1731, 15th AIAA Aerodynamic Decelerator Systems Technology Conference and Seminar, June 1999.

[7] Hur G., et al, *Identification of Powered Parafoil-Vehicle Dynamics from Modelling and Flight Test Data*, PhD dissertation, Texas A&M University, Texas, May 2005.

[8] Ward M., Costello M., and Slegers N., et al, *Specialized System Identification for Parafoil and Payload Systems*, Journal of Guidance, Control and Dynamics, April 2012.

[9] Gábor A., Villaverde A.F., and Banga J.R., *Parameter identifiability analysis and visualization in large-scale kinetic models of biosystems*, BMC Systems Biology, 11(54), 2017.

[10] Hur G. et al, *System Identification Of Powered Parafoil-Vehicle From Flight Test Data*, AIAA 2003-5539, Texas, 2003

[11] Strahan A. et al, *Testing of Parafoil Autonomous GN&C for X-38*, AIAA 2003-2115, California, 2003

[12] Jann T., et al, *Parafoil Test Vehicle ALEX - Further Development And Flight Test Results,* AIAA-99-1751, DLR, 1999

[13] Yakimenko O., et al, *Mobile System for Precise Aero Delivery with Global Reach Network Capability,* Proceedings of the 7th IEEE International Conference on Control & Automation, Christchurch, New Zealand, December 9-11, 2009